Engineered catalytic biofilms: Site-specific enzyme immobilization onto E. coli curli nanofibers

Engineered Catalytic Biofilms: Site-Specific Enzyme Immobilization onto *E. coli* Curli Nanofibers

Zsofia Botyanszki[1,3], Pei Kun R. Tay[2,3], Peter Q. Nguyen[2,3], Martin G. Nussbaumer[2,3], and Neel S. Joshi[2,3]*

Department of Chemistry and Chemical Biology[1],

School of Engineering and Applied Sciences[2],

Wyss Institute for Biologically Inspired Engineering[3],

Harvard University, Cambridge, MA 02138, USA.

*Corresponding Author: Dr. Neel S. Joshi

School of Engineering and Applied Sciences /

Wyss Institute for Biologically Inspired Engineering

Harvard University

Cambridge, MA 02138, USA.

Tel: (617) 432-7730

E-Mail: njoshi@seas.harvard.edu

Abstract

Biocatalytic transformations generally rely on purified enzymes or whole cells to perform complex transformations that are used on industrial scales for chemical, drug, and biofuel synthesis, pesticide decontamination and water purification. However, both of these systems have inherent disadvantages related to the costs associated with enzyme purification, the long-term stability of immobilized enzymes, catalyst recovery and compatibility with harsh reaction conditions. We developed a novel strategy for producing rationally designed biocatalytic surfaces based on Biofilm Integrated Nanofiber Display (BIND), which exploits the curli system of *E. coli* to create a functional nanofiber network capable of covalent immobilization of enzymes. This approach is attractive because it is scalable, represents a modular strategy for site-specific enzyme immobilization, and has the potential to stabilize enzymes under denaturing environmental conditions. We site-specifically immobilized a recombinant α-amylase, fused to the SpyCatcher attachment domain, onto *E. coli* curli fibers displaying complementary SpyTag capture domains. We characterized the effectiveness of this immobilization technique on the biofilms and tested the stability of immobilized α-amylase in unfavorable conditions. This enzyme-modified biofilm maintained its activity when exposed to a wide range of pH and organic solvent conditions. In contrast to other biofilm-based catalysts, which rely on cellular metabolism to remain active, the modified curli-based biofilm remained active even after cell death due to organic solvent exposure. This work lays the foundation for a new and versatile method of using the extracellular polymeric matrix of *E. coli* for creating novel biocatalytic surfaces.

45 Keywords: Biofilm, bacterial immobilization, curli fibers, biocatalysis, enzyme display,
46 extracellular matrix

Introduction

Biocatalysis provides an environmentally friendly alternative to chemical synthesis with its ability to perform complex chemical transformations in a scalable manner (Wohlgemuth, 2007). Enzymes are inherently attractive as catalysts due to their ability to perform chemo-, regio- and stereo-selective catalysis even on large, complex molecules. This fuels their use in the pharmaceutical industry and elsewhere, as alternatives to less selective synthetic chemical transformations (Murphy, 2012; Pollard and Woodley, 2007).

Enzymes can be used in purified form, in crude cell lysates, encased in synthetic protective materials such as a polymer matrix or lipid vesicle, or within whole cells. The attributes of these biocatalytic approaches have been extensively reviewed in the literature (Halan et al., 2012; Krishna, 2002; Pollard and Woodley, 2007; Rosche et al., 2009; Zhou and Hartmann, 2012). Whole cell catalysis is used widely in industry, however its production efficiency is limited by low mass transport stemming from hindered diffusion of the substrate or product across the cell membrane (Chen, 2007; Leon et al., 1998). Cell surface display methods have been explored in order to circumvent the problem of mass transport, but these approaches are hindered by the limited area on the bacterial cell surface and logistical difficulties in adapting the technique for multimeric enzyme complexes and multi-enzyme transformations (Daugherty, 2007; Löfblom, 2011; van Bloois et al., 2011). An approach that optimally combines the criteria of high surface area, enhanced enzyme stability, rapid mass transport, and modularity remains elusive.

Recently, our lab, and others, have explored a new immobilization surface on bacteria – the amyloid nanofibers of biofilms (Chen et al., 2014; Nguyen et al., 2014; Van Gerven et al., 2014). Biofilms are matrix-encapsulated bacteria adhered to each other and to surfaces or

interfaces (Costerton et al., 1995). Along with the other extracellular matrix components, these biosynthetic supramolecular polymers protect the cells against toxic chemicals, metals and physical stresses (Fang et al., 2002; Gross et al., 2010; Harrison et al., 2007), making biofilm-based materials well suited for industrial applications.

We developed a protein immobilization platform that modifies curli nanofibers, the amyloid fiber component of *E. coli* biofilms, with a peptide domain that can covalently capture proteins (Nguyen et al., 2014). In our approach, Biofilm Integrated Nanofiber Display (BIND), heterologous functional peptide domains are genetically fused to the amyloidogenic protein CsgA. When CsgA-peptide fusions assemble into curli fibers, the peptide domains become functional handles that can be used to modify the properties of the fibers, to capture metals, template nanoparticle growth or to enhance adhesion to surfaces. Recent advances in the engineering of this system have demonstrated that the curli pathway can be used to export a variety of CsgA-functional chimeras and also completely heterologous amyloidogenic sequences, suggesting that this could be a highly generalizable approach to functional materials synthesis (Chen et al., 2014; Nguyen et al., 2014; Sivanathan and Hochschild, 2012; Sivanathan and Hochschild, 2013; Van Gerven et al., 2014; Zhong et al., 2014).

In this work, we demonstrate that a large, industrially relevant enzyme, α-amylase, can be immobilized onto the curli fibers of *E. coli* biofilms, which we have termed catalytic-BIND (Figure 1). We used a genetically programmable, irreversible immobilization method – the spontaneous covalent bond formation between 13-amino acid SpyTag and 15 kDa SpyCatcher split protein (Zakeri et al., 2012). As previously shown, SpyTag fused to CsgA (CsgA-ST) assembles into fibers that closely resemble the native curli fibers with the SpyTag accessible for conjugation to SpyCatcher (Nguyen et al., 2014). When SpyCatcher is fused to α-amylase, the

immobilization reaction is robust, with the ability to form site-specific attachment between the two components, even in a complex mixture. We characterized the immobilization and activity of the enzyme on the biofilm using a filter plate assay and showed that α-amylase activity is retained after incubation in a range of pH and organic solvents, even when metabolic activity of the cells is disrupted. Our results suggest that this technology may be able to combine the scalability of whole cell catalysis with the modularity of enzyme surface immobilization through the transformation of *E. coli* biofilm extracellular matrices into designer functionalized surfaces.

Materials and Methods

Cell Strains, Plasmids and Reagents

All strains and vectors are listed in Supplementary Table I and II. *CsgA* and *csgA-SpyTag* genes were cloned into pBbE1a vectors. The csgA deletion mutant PHL628-*ΔcsgA (*MG1655 *malA-Kan ompR234 ΔcsgA* (Vidal et al., 1998)) used for biofilm experiments was a kind gift from the Hay Laboratory (Toba et al., 2011). CsgA was expressed in YESCA media, containing 10 g/L of casamino acids (Fisher, BP1424) and 1 g/L of yeast extract (Fisher, BP1422). YESCA plates also contained 15 g/L of agar. DPBS (LifeTechnologies, 14190-144) without calcium or magnesium was used as the general buffer for enzymatic reactions (abbrev. PBS). TBST (2.4g Tris base, 8.8g NaCl, 1 mL Tween-20, per L, pH 7.4-7.6) was used as wash buffer. Organic solvents were purchased from Sigma Aldrich, BDH Solvents, EMD, in >98% purity or HPLC grade. The *α-amylase* gene was isolated from *Bacillus licheniformis* ATCC 14580. *SpyCatcher* gene was acquired from Addgene (plasmid # 35044). α-Amylase was inserted at the N-terminus of SpyCatcher and the construct was subcloned into a pET28b vector (Novagen, 69865). Amylase-SpyCatcher (Amylase-SC) was expressed in Rosetta cells (Novagen, 70953) grown in Terrific Broth (Sigma T0918). Cells were lysed using a Misonix Probe Sonicator 4000. Millipore

PCF and hydrophilic PTFE filter plates (MSSLBPC10, MSRLN0410) and the Millipore MultiScreen vacuum manifold apparatus was used for filter plate assays. Amylase-SC was also immobilized onto His-Pur magnetic beads (LifeTechnologies, 88831). For amylase activity, 4-nitrophenyl-α-D-maltopentaoside (pNPMP, Sigma, 66068-38-0) was used as a substrate and recombinant purified α-amylase from *Bacillus licheniformis* (Sigma, A3403) as a standard. An iBlot Dry Blotting system (LifeTechnologies) was used for transferring gels to PVDF membranes (LifeTechnologies, IB4010). Anti-His antibody was purchased from Pierce Sci. (MA1-21315) and Western Blots were developed using Clarity ECL Substrate (BioRad, 170-5060). pH was measured using a Mettler Toledo FE20-Basic pH meter with an InLab®Routine probe. LC/MS/MS analysis was performed at the Taplin Mass Spectroscopy Facility. Scanning Electron Microscope (SEM) images were taken on a Zeiss Ultra Plus FESEM and confocal microscopy was performed on a Leica SP5 X MP Inverted Confocal Microscope.

Curli Expression

PHL628-*ΔcsgA* cells were transformed with either an empty pBbE1a plasmid or pBbE1a plasmids with CsgA, CsgA-ST, CsgATEVEKHis-ST (abr. CsgA[25AA]His-ST). The cells were then streaked onto YESCA plates with 100-200 μg/mL ampicillin. Transformed PHL628 cells were grown up in YESCA with ampicillin until an OD of 0.4-0.6 at 30°C. Curli expression was induced with 0.3 mM IPTG. Cultures were shaken for 18h-24h at 25°C and 150 rpm.

Quantitative Congo Red (CR) Binding Assays

Congo Red (CR) binding assay was adapted from previously published methods (Chapman, 2002). 1 mL of induced culture was pelleted at 5000g for 10 min and resuspended gently in PBS. Congo Red was added to 0.025 mM and allowed to incubate at 25°C for 10 min. The cells were then pelleted at 21,000g and the absorbance of the supernatant was measured at 490 nm in a

BioTek H1 microplate reader. The amount of CR binding was determined by subtracting the amount of this measurement from a PBS + CR control.

Amylase-SpyCatcher Expression

Rosetta cells transformed with pET28b Amylase-SC were grown up in overnight cultures in LB at 30°C with 100 μg/mL kanamycin. 1L of Terrific Broth was supplemented with kanamycin, inoculated with the overnight culture and grown up at 30°C until an OD of 0.4. Amylase-SC expression was induced with 0.5 mM IPTG and allowed to express overnight at 18°C. Cells were harvested and lysed in TBST and Amylase-SC was purified on a Ni-NTA column.

Amylase-SpyCatcher Activity Assay

4-Nitrophenyl-α-D-maltopentaoside (pNPMP) was chosen as the substrate to measure α-amylase activity because hydrolysis of 4-nitrophenol (pNP) from the pentasaccharide can be monitored at 405 nm. Note, the absorbance of pNP is dependent on its protonation state.

Curli Biofilm Assays

PHL628 biofilms expressing wild-type CsgA or CsgA-ST were cultured for 18h at 25°C at 150 rpm as described above. Curli content was measured using the quantitative CR binding assay. 50-100 μL of cells (normalized to CR absorption) were transferred onto filter plates, which were previously blocked with 0.5-2% BSA for at least 1.5h. For suspended biofilm assays, the biofilms were distributed into Eppendorf tubes and the same conjugation procedures followed. The media was filtered through using a vacuum manifold. Cells were washed with PBS or TBST. Cells were incubated with Amylase-SC in PBS with BSA or TBST overnight. To determine the remaining activity of the SpyCatcher on Amylase-SC that was left in solution after incubation, the filtrate was reacted with MBP-ST for 3h. The reaction mixture was concentrated, dissolved in 2x Laemmli buffer and a Western Blot run. For activity assays on the biofilm, the

conjugation mixture was removed using vacuum filtration and the biofilms were washed six times with 0.3% BSA in PBS or TBST over 90 min. For activity assays at different pH, 1.25 mM pNPMP in PBS was pH-ed with NaOH and HCl and added to the cells. Plates were placed on a desktop shaker and shaken at 150 rpm at room temperature for 1.5-2h. At the end of the experiment, the supernatant was vacuum filtered into a new 96-well plate, 5 M NaOH was added to increase pH to 12-14 (to bring pNP to a uniform protonation state) and pNP hydrolyzation was measured at 405 nm. For activity assays in organic solvents, biofilms were incubated with the solvents for 1-2h. The solvents were removed and cells washed with PBS. 1.25 mM pNPMP in PBS was added to the biofilm. Plates were placed on a desktop shaker at room temperature (rt). At the end of the experiment, the supernatant was vacuum filtered into a new 96-well plate and pNP release measured at 405 nm. In the data analysis, the reference activity is to pH 7 PBS. All data points are averages of reactions done in triplicate with error bars indicating standard deviation.

MTS Assay

Cell viability was tested using Promega CellTiter 96 Aqueous Non-Radioactive Cell Proliferation Assay. Functionalized biofilms were prepared as described above. Subsequent to exposure of biofilms to pH, miscible and immiscible organic solvents, biofilms were washed with PBS, incubated with assay buffer for 1h, filtered through and results read optically at 490 nm. In the data analysis, biofilms incubated in pH 7 PBS were used as the normalization for activity.

Results and Discussion

Amylase-SC Stability

We chose α-amylase as our model enzyme because of its wide use, industrial applicability, and the commercial availability of a water-soluble colorimetric substrate. The stability of α-amylase and its substrate also allowed us to correlate the observed enzyme activity to the stability of the biofilm as a whole, since we could assume that the enzyme would not degrade on the timescale of our experiments. While multiple proteins have been successfully attached to SpyCatcher (Fairhead et al., 2014; Nguyen et al., 2014; Schoene et al., 2014; Zakeri et al., 2012), this paper represents the first example of using the SpyTag and SpyCatcher fusions to immobilize an industry-relevant enzyme onto curli fibers. We designed a construct, named Amylase-SpyCatcher (abr. Amylase-SC), consisting of an α-amylase gene fused to the N-terminus of SpyCatcher via a 13 amino acid flexible linker. We confirmed that the fusion of the SpyCatcher domain to α-amylase had minimal impact on the kinetics of the two enzymes, and the difference in their stability over time and under a range of temperatures was negligible compared to the wild-type enzymes (Supplementary Figure 1 and Supplementary Table III).

Covalent Amylase-SC Attachment to Biofilms

We chose the SpyTag-SpyCatcher immobilization strategy because of its ability to form site-specific covalent bonds between the enzyme fusion proteins and the modified curli fibers, even in complex mixtures (Nguyen et al., 2014). This feature makes it particularly attractive because it obviates the need for time consuming and expensive enzyme purification efforts. In order for this strategy to be effective, the SpyTag domain must remain sufficiently accessible after amyloid assembly to participate in covalent bond formation. We confirmed that covalent conjugation between Amylase-SC and fully formed curli fibers displaying SpyTag was feasible

205 through a SDS-PAGE gel shift assay and subsequent LC/MS/MS analysis (Supplementary
206 Figure 2 and Supplementary Table IV).

207 A filter plate-based assay was used to assess the catalytic potential of the curli-
208 immobilized enzymes under a variety of conditions. Cells were grown in culture and induced to
209 produce recombinant CsgA before being transferred onto 96-well filter plates. Confocal
210 microscopy and scanning electron microscopy (Figure 2) revealed that the filter surface was
211 coated with one to two layers of cells surrounded by a thick mat of extracellular material. DAPI
212 staining of cells throughout the mass of the biofilm, done previous to sample drying for SEM
213 analysis, suggests that it is porous enough that small molecules can permeate it in the hydrated
214 state. In order to determine whether the filtration process resulted in lower SpyTag accessibility,
215 Amylase-SC was reacted overnight with either filter plate immobilized cells or suspended cells
216 after curli induction from a strain that secretes CsgA with a short, 6 amino acid, linker to ST
217 (CsgA-ST) and one with a 31 amino acid linker to ST (CsgA[25AA]His-ST). As shown in
218 Figure 3, the activity resulting from these two immobilization techniques after overnight
219 incubation was similar. This indicates that filtration does not affect the availability of the SpyTag
220 sites under these experimental conditions and longer incubation times. This is reasonable, since
221 the protocol yields essentially a monolayer of cells with their extracellular material surrounding
222 them. If thicker biofilms are used, the issue of enzyme-SC diffusivity will need to be further
223 investigated.

224 SpyCatcher conjugation is known to proceed rapidly in homogeneous solution, with the
225 conjugation reaction effectively complete within a half hour under a variety of conditions (Zakeri
226 et al., 2012). However, since the SpyTag domain is displayed in a dense array on the surface of
227 the curli fibers, we wanted to compare the kinetics of the Amylase-SC conjugation reaction

between soluble and fiber-bound SpyTag. Accordingly, we reacted purified Amylase-SC with either a soluble protein, maltose binding protein, fused to SpyTag (abr. MBP-ST) or SpyTag displayed on fully assembled fibers in suspension culture. The gel shown in Supplementary Figure 3 illustrates that essentially all Amylase-SC reacts with MBP-ST within 10 minutes, indicating that the presence of the α-amylase does not hinder accessibility to SpyCatcher's active site, nor does it significantly alter SpyCatcher's reaction kinetics. Next, we monitored the kinetics of the conjugation reaction performed in suspension with CsgA-ST and CsgA[25AA]His-ST. The results, shown in Figure 4, illustrate that Amylase-SC binding to the biofilms on filter plates is much slower than in solution – on the order of hours to days instead of minutes. The construct with the longer linker exhibited significantly faster conjugation kinetics (36 hours to maximum product formation) compared to the shorter linker construct, suggesting that SpyTag accessibility may be a parameter worth optimizing in order to increase conjugation efficiencies for future efforts.

There may be several reasons to explain the extended times needed for conjugation to the biofilms (Figure 4). One possibility is a degradation of the SpyCatcher protein. To test this, Amylase-SC that remained unattached after being incubated with biofilms expressing CsgA, CsgA-ST and CsgA[25AA]His-ST for 56h was removed and reacted with MBP-ST. The Western Blot in Supplementary Figure 4 confirms that even after incubation of this length, the SpyCatcher protein is able to conjugate to MBP-ST in solution, eliminating this as a possible explanation. Instead, increased diffusion distances may be responsible for the slower reaction. In biofilms, enzymes need to diffuse to the surface, which is a much larger distance on average than diffusing to a uniformly distributed MBP-ST. Indeed, binding to curli expressing cells in suspension is faster than binding to filter plate immobilized cells (Supplementary Figure 5). In

addition, Amylase-SC (72 kDa) is significantly larger than the CsgA-ST monomer (15 kDa), and since the actual surface is a polymer of self-assembled CsgA-STs, both the core curli fiber and previously immobilized Amylase-SCs may sterically hinder the conjugation of free Amylase-SC on neighboring SpyTag sites. This may explain why the CsgA[25AA]His-ST expressing biofilms can bind Amylase-SC faster.

Correlating Congo Red Adsorption to Enzyme Immobilization

We expected that the amount of curli being produced by the cells would be a good predictor for the amount of enzyme that could be immobilized. We therefore attempted to correlate amyloid production, as measured by CR staining, with enzyme immobilization. Although CR staining can be problematic because of nonspecific staining of other proteins and biopolymers, we confirmed that this was not a problem for the *E. coli* strain we used for these experiments by demonstrating a lack of staining for cells transformed with an empty plasmid that did not contain the gene encoding CsgA (Nguyen et al., 2014). We also investigated whether CR staining is dependent on the amount of non-curli biomass in the sample. To do this, we diluted CsgA[25AA]His-ST expressing PHL628 cells with PHL628 cells that do not express curli and measured CR binding. The linear relationship observed for this curli concentration curve (Supplementary Figure 6) indicates that the CR binding to curli is not blocked by the presence of extra cells.

To correlate curli production to activity, we compared the CR binding to the Amylase activity on the fibers of filter plate immobilized cells. As shown in Figure 5, there is a linear correlation between CR adsorbed and the activity of the enzymes (reported as pNP hydrolyzed). This linearity indicates that CR binding appears to be a valid measure of the relative amount of

enzyme immobilized, although absolute measurements of the immobilized enzyme concentration remain elusive.

Enzyme activity measurement in solution and on filter plates

In order to determine how the amount of Amylase-SC in the stock solution (reaction mixture) affected immobilization, we incubated filter plate immobilized cells with a range of concentrations of Amylase-SC. The resulting activity, shown in

279 Figure 5 Product hydrolyzed as a function of Congo Red captured by the CsgA-ST biofilms.

280 Dotted lines are present for guidance and show the best fit of the data (R^2=0.93). The quantity of

281 pNP hydrolyzed was recorded after 85 min incubation with 100µL of 1.25 mM pNPMP at 150

282 rpm. Error bars show SD for n=3.

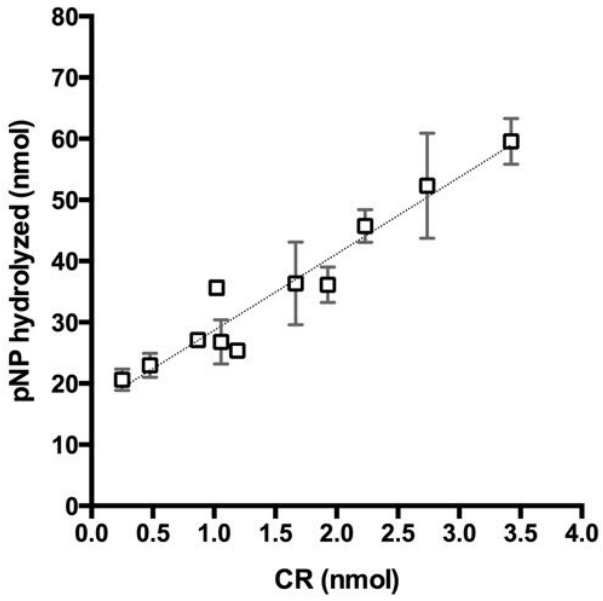

283

284

Figure 6, illustrates a linear increase with the amount of Amylase-SC concentration. Despite normalizing both cell cultures to CR, there is a difference between the activity seen on the CsgA-ST and CsgA[25AA]His-ST displaying cells because the reaction was not fully at completion. When we converted the values for hydrolyzed pNP concentration to the amount of soluble enzymes needed to hydrolyze that much pNP (the effective enzyme concentration at this shaking speed) we found that at the highest Amylase-SC concentration in Figure 6, 6 and 12% (CsgA-ST and CsgA[25AA]His-ST respectively) of the enzyme activity of the stock solution was observed. Since the bulk kinetics on a catalytic surface for a neutral substrate are generally slower than in a well mixed solution(Bommarius and Riebel-Bommarius, 2007; Hornby and Lilly, 1968; Kobayashi and Laidler, 1973)(Supplementary Figure 7), the effective enzyme concentration calculated this way provides us with a minimum estimate for the amount of enzyme immobilized.

Biofilm Immobilized Amylase-SC Activity as a Function of pH

For the successful use of catalytic biofilms in many synthetic and environmental applications, they may need to withstand a range of conditions that are not normally conducive for bacterial growth or enzyme stability. Many enzymes used in industry today have been engineered specifically to enhance their stability under extreme pH conditions, high temperatures, and in the presence of detergents and organic solvents (Bommarius and Paye, 2013; Kirk et al., 2002). Previous characterization experiments showed that α-amylase is fully active in pH range 5-9 (Nielsen et al., 2001). As shown in Figure 7A, Amylase-SC immobilized onto the biofilms maintained full activity for the pH 5-9 range, but also showed full activity at pH 4 and pH 10, even though the soluble Amylase-SC lost 40% of its activity at those pH values. The cells show a slightly increased metabolic activity from pH 3-6, which is likely due to stress response to the unfavorable pH and buffer conditions (Figure 7B).

Amylase-SC Stability on Biofilms Incubated with Organic Solvents

Biocatalytic systems that are able to catalyze reactions on compounds with low water solubility are of particular interest in industry. Most existing methods designed to circumvent the issue of water solubility use two-phase aqueous-organic systems. In these systems, the organic soluble molecule briefly enters the aqueous phase, where the enzyme is able to catalyze the reaction, and then exits again into the organic phase (Hertzberg et al., 1992; Kawakami et al., 1990; Sinisterra and Dalton, 1996). Laane et. al. proposed a positive correlation between reactivity and the logarithm of the partitioning coefficient (logP) of the organic solvent (Laane et al., 1987). Water-miscible solvents have a logP<0, polar organic solvents have a logP<2 and nonpolar solvents have a logP>2. For whole cell catalysts, solvents that are non-polar enough to have a logP between 2-5 (depending on cell type) or greater are able to maintain catalytic activity. The loss of activity is believed to be due to inactivation of enzymes, the breakdown of transport mechanisms, disruption of the cell membrane by the solvent and cell lysis that results from exposure to the organic solvents (Leon et al., 1998).

We hypothesized that the enzyme-functionalized biofilms would be able to withstand some exposure to non-miscible organic solvents because biofilms should remain hydrated under such conditions and hence prevent the denaturation of immobilized enzymes. To test this hypothesis, we incubated Amylase-SC conjugated biofilms with a panel of water-miscible and non-miscible organic solvents. Since pNPMP is not soluble in most organic solvents, we first incubated the biofilms in the organics and then replaced the solvent with PBS while measuring activity. As shown in Figure 8A, the relative activity of immobilized Amylase-SC is only slightly affected by incubation with non-miscible solvents, but completely disappears in miscible solvents. Miscible solvents can access and denature the enzymes, and may disrupt curli fiber assembly or anchoring, while a hydration layer separates the non-miscible solvents. Plotting the

results in Figure 8A against the partitioning coefficient of the solvents, Figure 8B shows that Amylase-SC activity is mostly preserved when biofilms are incubated in solvents with logP>0. Notably, 70-90% activity is retained for biofilms incubated in solvents with logP 0.6-0.8, while in the whole cell systems documented in the literature, the use of these solvents resulted in little to no activity for whole cell catalysts (Laane et al., 1987). Indeed, the metabolic activity of the cells following organic solvent exposure shows that cell metabolism ceased in all solvents tested except decane, which has a logP of 5.6 (Figure 8C). This correlates with the results previously mentioned for whole cell catalysis in two-phase systems. Although direct comparisons to the soluble enzyme was not possible in this case due to the insolubility of the enzyme substrate in organics, Amylase-SC does show similar organic solvent tolerance when immobilized onto Ni-NTA beads (Supplementary Figure 8). Further information using other enzyme systems will be needed to definitively establish the impact of the biofilm on enzyme stability. However, operability at the logP 0-2 range may be a unique feature to our system that is afforded by the fact that despite our use of cells, the catalytic component of our system does not rely on cell viability.

It is also worth noting that we chose the PHL628 strain for these experiments specifically because curli fibers are the only extracellular polymer that it produces, which simplified the characterization experiments. However, for future studies, long term enzyme stability might benefit from the use of strains that produce other extracellular polymers (i.e. cellulose and other pili) that can serve a protective role for the immobilized enzymes.

Biofilm stability over time

The stability of the catalytic system is very important in industrial applications of catalytic technologies, since cost savings can be achieved by the extended use of immobilized catalysts, thus reducing reactor downtime (Halan et al., 2012). While our filter plate setup cannot

be used to determine the stability of the biofilms under flow or batch processing conditions, we investigated the stability of the Amylase-SC attached to the biofilm over time. Amylase activity was retested after a period of 28 days with the filter plate immobilized biofilm kept at 4^{o}C in buffer. Figure 9 shows that the biofilms displayed the same level of activity after the 12 days with a slight decrease after 28 days, indicating that the biofilm and its entangled curli fibers were stable enough that the fibers were not displaced through the filter during the vacuum-assisted washing steps.

Conclusions

In this work, we demonstrated a novel platform for the immobilization of enzymes onto the extracellular matrix of an engineered biofilm. We were able to create biofilms displaying functional biochemical handles on the curli network of *E. coli*. Subsequently the SpyTag-SpyCatcher immobilization strategy was used to site-specifically conjugate α-amylase to the biofilms, which revealed that enzymes remained active after exposure to various adverse conditions.

There are several attractive features of this biofilm-based material compared to other surfaces for enzyme immobilization: (1) the conjugation strategy we employ proceeds spontaneously, without the need for any chemical treatment steps, and provides a simple, modular way to immobilize enzymes site-specifically to surfaces; (2) the conjugation sites are densely arrayed on the curli fibers, producing a high surface area for immobilization; (3) the material is produced entirely biosynthetically, which is a green alternative to petroleum-derived synthetic polymers.

This technology could be combined with more established biofilm-based biocatalytic processes (Gross et al., 2010; Halan et al., 2010; Karande et al., 2014) to yield stable biofilms in flow reactors that are able to catalyze reactions not accessible to currently available whole cell

1 catalyst systems. Furthermore, we have previously demonstrated the potential for creating
2 multifunctional BIND materials (Nguyen, at al., 2014), suggesting that the engineered curli
3 fibers could be used for immobilizing multiple enzymes for multi-step transformations, or for
4 combing catalysis with other functions that may be attractive in the context of a bioreactor, like
5 substrate adhesion. This would be useful in many forms of 'green' biocatalysis, including in
6 pharmaceutical synthesis, breakdown of pharmaceuticals in wastewater, removal of
7 contaminants from groundwater or the creation of catalytic surfaces for bioenergy production.

Acknowledgements

This work was funded by the Wyss Institute for Biologically Inspired Engineering. Z.B. acknowledges NSF GRF for funding and P.R.T for funding from A*STAR National Science Graduate Fellowship (Singapore). We thank Prof. Anthony G. Hay (Cornell Univ.) for providing the PHL628-*ΔcsgA* strain.

References

Bommarius AS, Paye MF. 2013. Stabilizing biocatalysts. Chem. Soc. Rev. **42**:6534.

Bommarius AS, Riebel-Bommarius BR. 2007. Biocatalysis. John Wiley & Sons 1 pp.

Chapman MR. 2002. Role of Escherichia coli Curli Operons in Directing Amyloid Fiber Formation. Science **295**:851–855.

Chen AY, Deng Z, Billings AN, Seker UOS, Lu MY, Citorik RJ, Zakeri B, Lu TK. 2014. Synthesis and patterning of tunable multiscale materials with engineered cells. Nature Materials **13**:515–523.

Chen RR. 2007. Permeability issues in whole-cell bioprocesses and cellular membrane engineering. Appl Microbiol Biotechnol **74**:730–738.

Costerton JW, Lewandowski Z, Caldwell DE, Korber DR, Lappin-Scott HM. 1995. Microbial biofilms. Annual Reviews in Microbiology **49**:711–745.

Daugherty PS. 2007. Protein engineering with bacterial display. Current Opinion in Structural Biology **17**:474–480.

Fairhead M, Veggiani G, Lever M, Yan J, Mesner D, Robinson CV, Dushek O, van der Merwe PA, Howarth M. 2014. SpyAvidin Hubs Enable Precise and Ultrastable Orthogonal Nanoassembly. J. Am. Chem. Soc. **136**:12355–12363.

Fang HHP, Xu L-C, Chan K-Y. 2002. Effects of toxic metals and chemicals on biofilm and biocorrosion. Water Research **36**:4709–4716.

Gross R, Lang K, Bühler K, Schmid A. 2010. Characterization of a biofilm membrane reactor and its prospects for fine chemical synthesis. Biotechnol. Bioeng. **105**:705–717.

Halan B, Buehler K, Schmid A. 2012. Biofilms as living catalysts in continuous chemical syntheses. Trends in Biotechnology **30**:453–465.

Halan B, Schmid A, Buehler K. 2010. Maximizing the productivity of catalytic biofilms on solid supports in membrane aerated reactors. Biotechnol. Bioeng. **106**:516–527.

Harrison JJ, Ceri H, Turner RJ. 2007. Multimetal resistance and tolerance in microbial biofilms. Nature Reviews Microbiology **5**:928–938.

Hertzberg S, Kvittingen L, Anthonsen T, Skjaak-Braek G. 1992. Alginate as immobilization matrix and stabilizing agent in a two-phase liquid system: application in lipase-catalysed reactions. Enzyme and Microbial Technology **14**:42–47.

Hornby WE, Lilly MD. 1968. Some changes in the reactivity of enzymes resulting from their chemical attachment to water-insoluble derivatives of cellulose. Biochem. J. **107**:669–674.

Karande R, Halan B, Schmid A, Buehler K. 2014. Segmented flow is controlling growth of catalytic biofilms in continuous multiphase microreactors. Biotechnol. Bioeng. **111**:1831–1840.

Kawakami K, Tsuruda S, Miyagi K. 1990. Immobilization of Microbial Cells in a Mixed Matrix of Silicone Polymer and Calcium Alginate Gel: Epoxidation of 1-Octene by Nocardia corallina B-276 in Organic Media. Biotechnol Progress **6**:357–361.

Kirk O, Borchert TV, Fuglsang CC. 2002. Industrial enzyme applications. Current Opinion in Biotechnology **13**:345–351.

Kobayashi T, Laidler KJ. 1973. Kinetic analysis for solid-supported enzymes. Biochim. Biophys. Acta **302**:1–12.

Krishna SH. 2002. Developments and trends in enzyme catalysis in nonconventional media. Biotechnology Advances **20**:239–267.

Laane C, Boeren S, Vos K, Veeger C. 1987. Rules for optimization of biocatalysis in organic solvents. Biotechnol. Bioeng. **30**:81–87.

Leon R, Fernandes P, Pinheiro HM, Cabral J. 1998. Whole-cell biocatalysis in organic media. Enzyme and Microbial Technology **23**:483–500.

Löfblom J. 2011. Bacterial display in combinatorial protein engineering. Biotechnology Journal **6**:1115–1129.

Murphy CD. 2012. The microbial cell factory. Org. Biomol. Chem. **10**:1949.

Nguyen PQ, Botyanszki Z, Tay PKR, Joshi NS. 2014. Programmable biofilm-based materials from engineered curli nanofibres. Nat Commun **5**:4945.

Nielsen JE, Borchert TV, Vriend G. 2001. The determinants of α-amylase pH–activity profiles. Protein Eng. **14**:505–512.

Pollard DJ, Woodley JM. 2007. Biocatalysis for pharmaceutical intermediates: the future is now. Trends in Biotechnology **25**:66–73.

Rosche B, Li XZ, Hauer B, Schmid A, Buehler K. 2009. Microbial biofilms: a concept for industrial catalysis? Trends in Biotechnology **27**:636–643.

Schoene C, Fierer JO, Bennett SP, Howarth M. 2014. SpyTag/SpyCatcher Cyclization Confers Resilience to Boiling on a Mesophilic Enzyme. Angew. Chem. Int. Ed. **53**:6101–6104.

Sinisterra JV, Dalton H. 1996. Influence of the immobilization methodology in the stability and activity of P. putida UV4 immobilized whole cells. Immobilized Cells: Basics and Applications: Basics and Applications **11**:416.

Sivanathan V, Hochschild A. 2012. Generating extracellular amyloid aggregates using E. coli cells. Genes & Development **26**:2659–2667.

Sivanathan V, Hochschild A. 2013. A bacterial export system for generating extracellular amyloid aggregates. Nature Protocols **8**:1381–1390.

Toba FA, Thompson MG, Campbell BR, Junker LM, Rueggeberg KG, Hay AG. 2011. Role of DLP12 lysis genes in Escherichia coli biofilm formation. Microbiology **157**:1640–1650.

van Bloois E, Winter RT, Kolmar H, Fraaije MW. 2011. Decorating microbes: surface display ofproteins on Escherichia coli. Trends in Biotechnology **29**:79–86.

Van Gerven N, Goyal P, Vandenbussche G, De Kerpel M, Jonckheere W, De Greve H, Remaut H. 2014. Secretion and functional display of fusion proteins through the curli biogenesis pathway. Molecular Microbiology **91**:1022–1035.

Vidal O, Longin R, Prigent-Combaret C, Dorel C, Hooreman M, Lejeune P. 1998. Isolation of an Escherichia coli K-12 mutant strain able to form biofilms on inert surfaces: involvement of a new ompR allele that increases curli expression. Journal of Bacteriology **180**:2442–2449.

Wohlgemuth R. 2007. Modular and scalable biocatalytic tools for practical safety, health and environmental improvements in the production of speciality chemicals. Biocatal Biotransformation **25**:178–185.

Zakeri B, Fierer JO, Celik E, Chittock EC, Schwarz-Linek U, Moy VT, Howarth M. 2012. Peptide tag forming a rapid covalent bond to a protein, through engineering a bacterial adhesin. Proceedings of the National Academy of Sciences **109**:E690–E697.
Zhong C, Gurry T, Cheng AA, Downey J, Deng Z, Stultz CM, Lu TK. 2014. Strong underwater adhesives made by self-assembling multi-protein nanofibres. Nature Nanotechnology:1–9.
Zhou Z, Hartmann M. 2012. Recent Progress in Biocatalysis with Enzymes Immobilized on Mesoporous Hosts. Top Catal **55**:1081–1100.

List of Figures

Figures

Figure 1 Catalytic-BIND: biofilm functionalization with enzymes through the covalent modification of curli fibers. **A** *E. coli* expresses CsgA fused to the 13 amino acid SpyTag (CsgA-ST), which self-assembles into curli fibers on the surface of the bacterium. When the bacteria form biofilms, curli fibers expressing SpyTag create a polymer matrix around the cells. **B** This polymer matrix is covalently modified with an enzyme fused to SpyCatcher. **C** Substrate to product catalysis occurs on the high surface-area catalytic fibers. pNPMP is 4-Nitrophenyl-α-D-maltopentaoside and R is the hydrolyzed α-D-maltopentaoside in the figure.

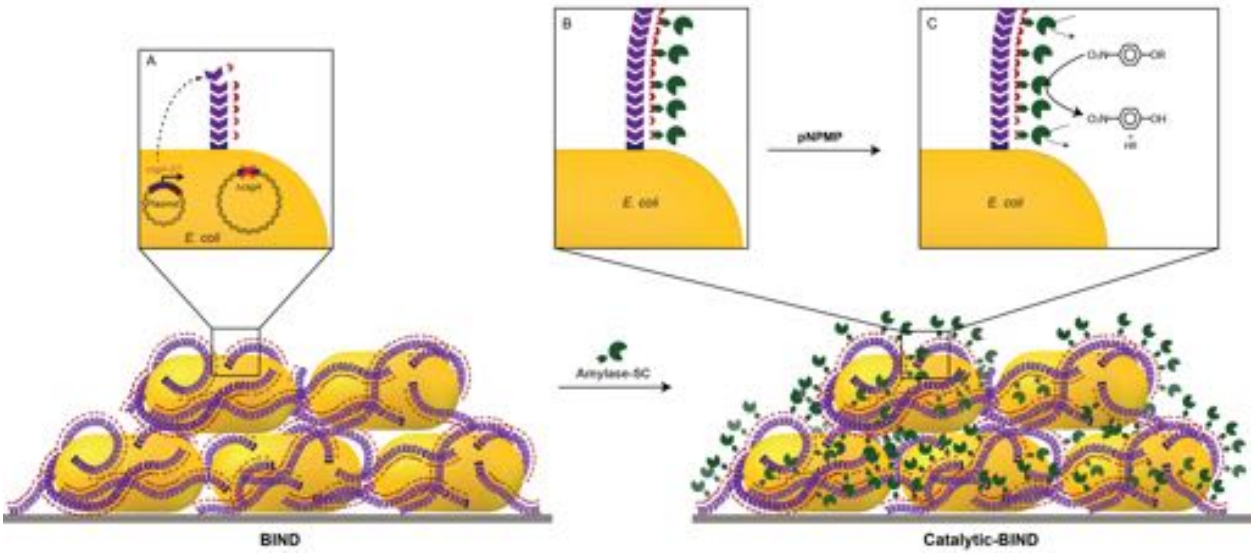

159 Figure 2 Biofilms immobilized on a 96-well filter plate. **A&C**. Wild-type CsgA and **B&D** CsgA-

160 ST expressing PHL628 cells visualized with fluorescence microscopy DAPI stain and SEM.

161 Scale bar for confocal images is 10 μm and 1 μm for SEM.

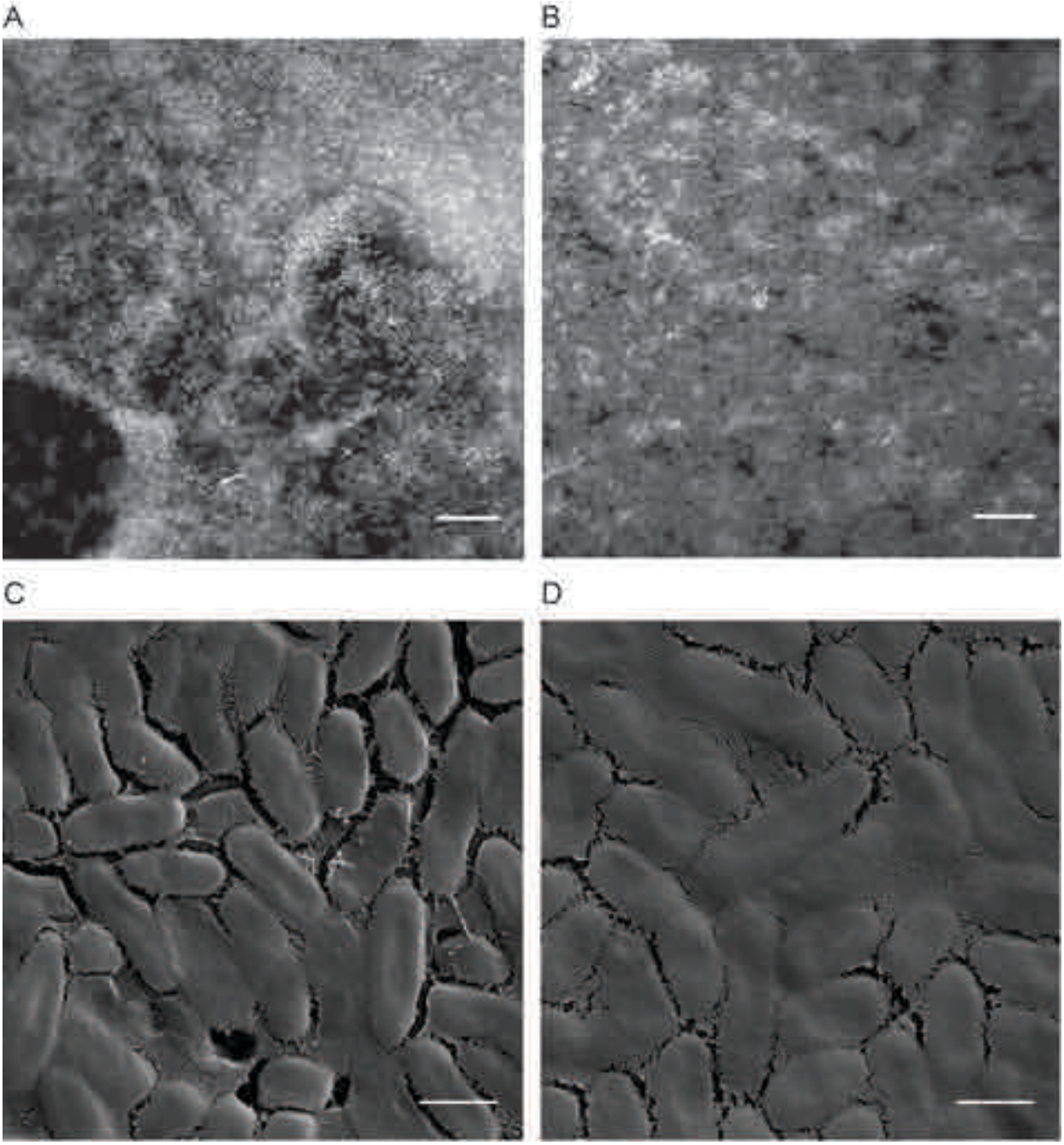

162

163

Figure 3 Parallel immobilization of Amylase-SC on biofilms displaying CsgA-ST suspended in solution (S) and immobilized on filter plates (FP). Samples were taken after 20h of immobilization. Suspended biofilms were filtered onto the filter plates so that the activity of all biofilms was measured under identical conditions. The quantity of pNP hydrolyzed was recorded after 260 min incubation with 100µL of 1.25 mM pNPMP at 150 rpm. Error bars show SD for n=3.

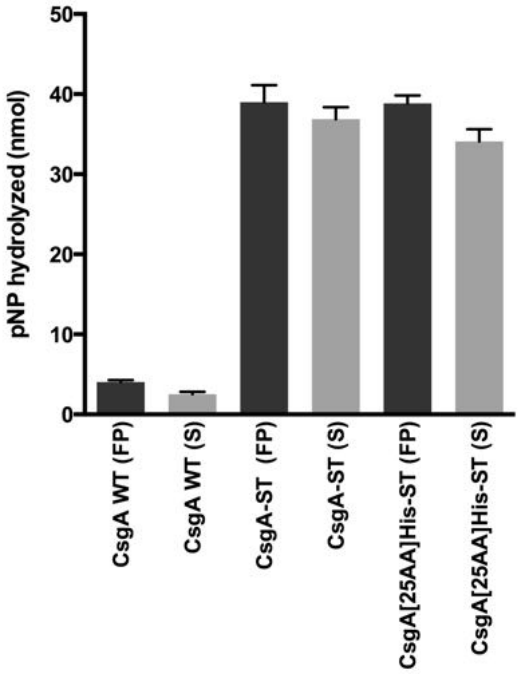

Figure 4 The binding of Amylase-SC to filter plate immobilized wild-type CsgA, CsgA-ST and CsgA[25AA]His-ST cells over a 110h incubation. Dotted lines connect adjacent time points for clarity. The quantity of pNP hydrolyzed was recorded after 105 min incubation with 100µL of 1.25 mM pNPMP at 150 rpm. Error bars show SD for n=3.

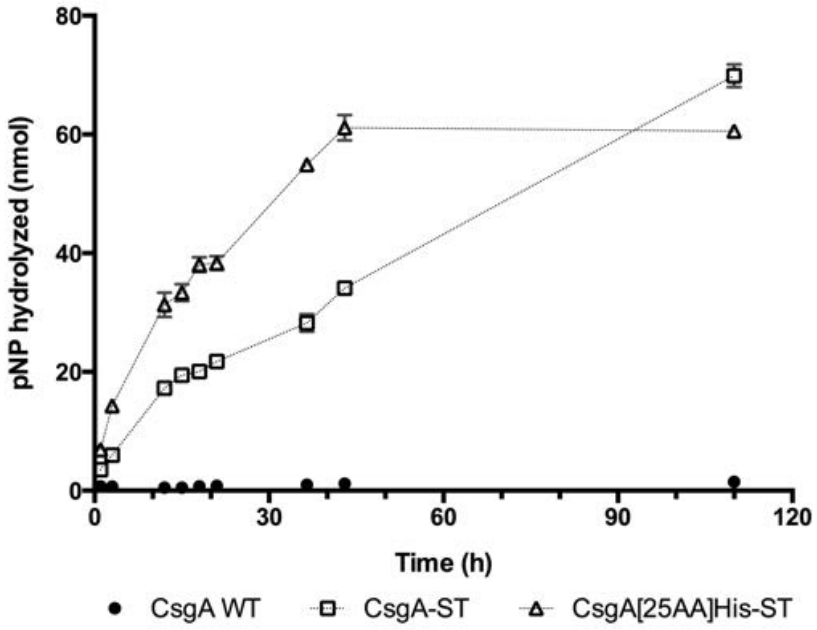

178 Figure 5 Product hydrolyzed as a function of Congo Red captured by the CsgA-ST biofilms.

179 Dotted lines are present for guidance and show the best fit of the data (R^2=0.93). The quantity of

180 pNP hydrolyzed was recorded after 85 min incubation with 100µL of 1.25 mM pNPMP at 150

181 rpm. Error bars show SD for n=3.

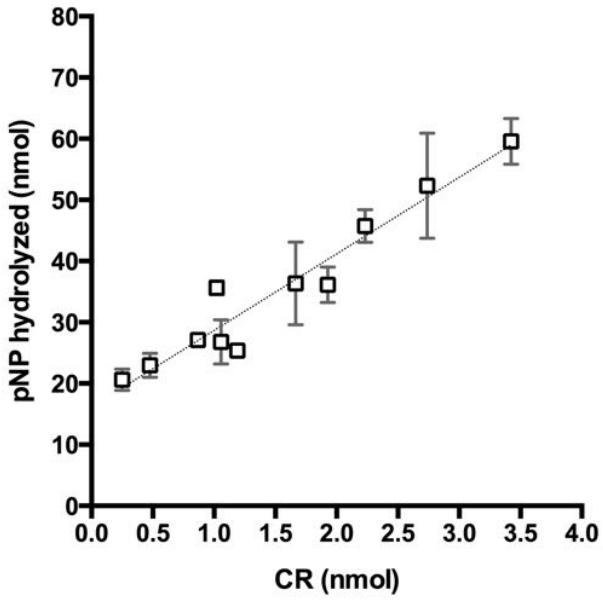

182

Figure 6 Activity of Amylase-SC on biofilms with respect to Amylase-SC in stock solution. AmylaseSC of varying concentrations was incubated with the biofilms. Dotted lines show the calculated best fit (R^2=0.78 for CsgA-ST and R^2=0.92 for CsgA[25AA]His-ST). The quantity of pNP hydrolyzed was recorded after 85 min incubation with 100µL of 1.25 mM pNPMP at 150 rpm. Error bars show SD for n=3.

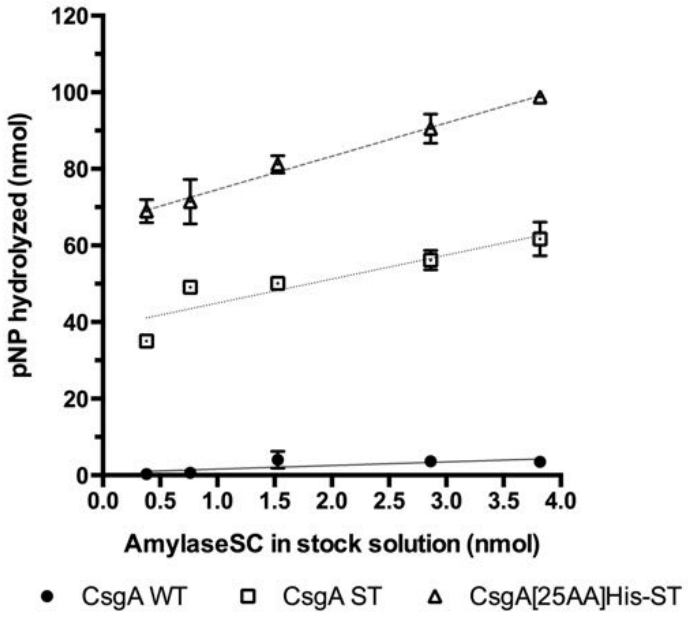

Figure 7 Amylase-SC stability and biofilm viability under a range of pH conditions. **A** pNP hydrolyzed by biofilm-immobilized Amylase-SC after incubation with buffers pH 2-12 for 2h compared to non-immobilized Amylase-SC. **B** Metabolic activity of cells post incubation in the panel of solvents. Values are shown relative to pH 7 PBS.

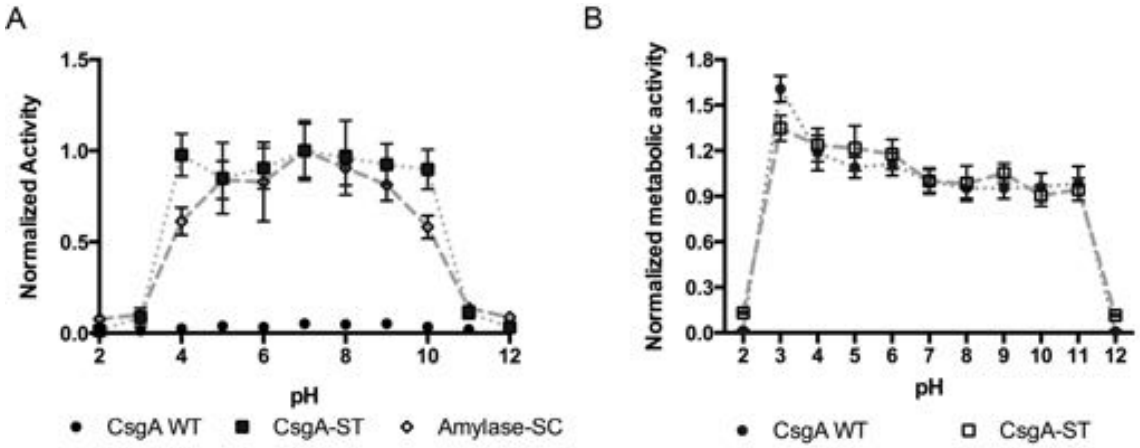

198 Figure 8 Amylase-SC stability and biofilm viability after incubation in organic solvents. **A** pNP

199 hydrolyzed by biofilm-immobilized Amylase-SC after incubation in panel of solvents for 2h. **B** Activity in **A** plotted against the log of the partition coefficient of the organic solvents. **C** Metabolic activity of cells post incubation in the panel of solvents. Values are shown relative to pH 7.

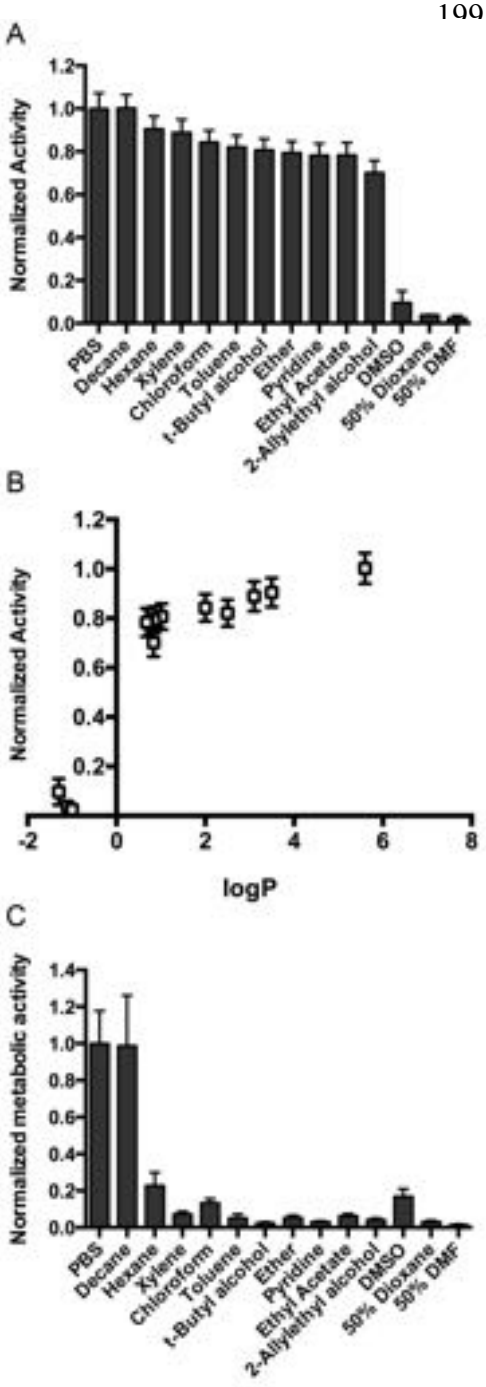

Figure 9 Stability of Amylase-SC on filter plate immobilized biofilms after 28 days. pNP reading was taken after 260 min incubation with 100µL of 1.25 mM pNPMP at 150 rpm. Error bars show SD for n=3.